Ellipsometric study of the electronic band structure of CrO_2 across the ferromagnetic transition

M. K. Stewart,[1,*] K. B. Chetry,[2] B. Chapler,[1] M. M. Qazilbash,[1] A. A. Schafgans,[1] A. Gupta,[2] T. E. Tiwald,[3] and D. N. Basov[1]

[1]*Department of Physics, University of California–San Diego, La Jolla, California 92093, USA*

[2]*Center for Materials for Information Technology, University of Alabama, Tuscaloosa, Alabama 35487, USA*

[3]*J. A. Woollam Company, Incorporated, 645 M Street, Suite 102, Lincoln, Nebraska 68508, USA*

(Received 12 January 2009; revised manuscript received 2 March 2009; published 15 April 2009)

The optical properties of half-metallic CrO_2 at temperatures below, at, and above the Curie temperature are studied by means of variable angle spectroscopic ellipsometry. The films were epitaxially grown on (100)- and (110)-oriented TiO_2 substrates by chemical vapor deposition. Optical conductivity data reveal a pronounced anisotropy of the optical constants for all films which is in good agreement with what is known about their crystal structure. The main features of the conductivity spectra in the ferromagnetic state are consistent with existing band-structure calculations. However, no temperature dependence of these features across the ferromagnetic transition is evident, posing questions about the electronic structure of the material.

DOI: 10.1103/PhysRevB.79.144414 PACS number(s): 75.50.Cc, 71.20.Be, 78.20.−e, 78.30.−j

I. INTRODUCTION

According to band-structure calculations CrO_2 is classified as a half-metallic ferromagnet with complete spin polarization at the Fermi energy.[1–3] This has sparked a renewed interest in this material as a candidate for spin injection in spintronic applications. The prediction has been confirmed by point contact Andreev reflection measurements showing 96–98 % spin polarization.[4,5] Other experiments such as x-ray absorption,[6] photoemission,[7] and optical measurements[8] performed below the Curie temperature show general agreement with band-structure calculations in the ferromagnetic state. Work done to study the electromagnetic response of this material across the ferromagnetic transition is limited to absorption[9,10] and pump-probe transmission[11] studies claiming to confirm a double-exchange mechanism of the ferromagnetic state. Within this latter scenario, major changes in the optical conductivity are expected across the ferromagnetic transition.[12] A comprehensive study of the optical properties across T_C in both the *c* axis and *ab* plane directions should help further our understanding of this half-metal. While it is well known that the crystal structure of CrO_2 is anisotropic,[13] experimental studies of the anisotropy in the optical response of thin films are also very limited.[11,14]

In this paper, we study the frequency-dependent optical conductivity of CrO_2 over a wide temperature and energy range in order to learn about its electronic band structure and carrier dynamics across the ferromagnetic transition. We employed variable angle spectroscopic ellipsometry (VASE): a technique that allows us to extract both the real and imaginary parts of the optical conductivity without recourse to Kramers-Kronig analysis.

II. EXPERIMENTAL METHODS

The samples are epitaxial CrO_2 thin films grown on TiO_2 substrates by chemical vapor deposition with CrO_3 as a precursor. Sample growth and characterization using x-ray diffraction, Rutherford backscattering spectroscopy, several microscopy techniques, and a standard four-probe dc method are described elsewhere.[15–17] We used two different samples: one deposited on TiO_2 in the (100) orientation with a thickness of 175 nm and one in the (110) orientation, 150 nm thick. The (100) film is strained while the (110) film is strain-free.[16–18] The reported Curie temperature of these films is T_C=390–395 K and the magnetic easy axis is the *c* axis.[15]

We performed the measurements using two commercial Woollam ellipsometers. One, a VASE model based on a grating monochromator, covers the energy range between 0.6 and 6 eV, to which we added a UHV cryostat in order to enable measurements at both low and elevated temperatures.[19,20] The other one, an IR-VASE model, covers the range between 0.05 and 0.7 eV and is based on a Michelson interferometer (Bruker 66vs). We first characterized the blank (100) and (110) substrates and then the films. Knowing that the crystal structure of CrO_2 is elongated along the *c* direction, it is natural to expect the electronic properties to be anisotropic.[11] In order to study the optical constants in the various crystallographic directions, it was necessary to measure the samples in two orientations: with the *c* axis in the plane of incidence and perpendicular to it. A schematic of these experimental geometries is shown in Fig. 1. Each measurement was performed at incidence angles of 60° and 75° and at temperatures ranging from 300 to 450 K, while some measurements in the visible and ultraviolet regions were extended down to 60 K. At each angle we measured the polarization state of the reflected light in the form of two parameters Ψ and Δ, as shown in Fig. 1, which are related to the Fresnel reflection coefficients for *p*- and *s*-polarized light (R_p and R_s) through the equation $\frac{R_p}{R_s}=\tan(\Psi)e^{i\Delta}$. We note that there is good agreement, better than 3%, between the data obtained from the two different ellipsometers in the overlapping frequency range.

In order to obtain the optical constants of the thin film samples, we first constructed a two-layer model taking proper account of the role of the substrate in raw ellipsometric data. The complex dielectric functions of the TiO_2 required for this analysis were determined through ellipsometric measurements of the bare substrates, keeping in mind the

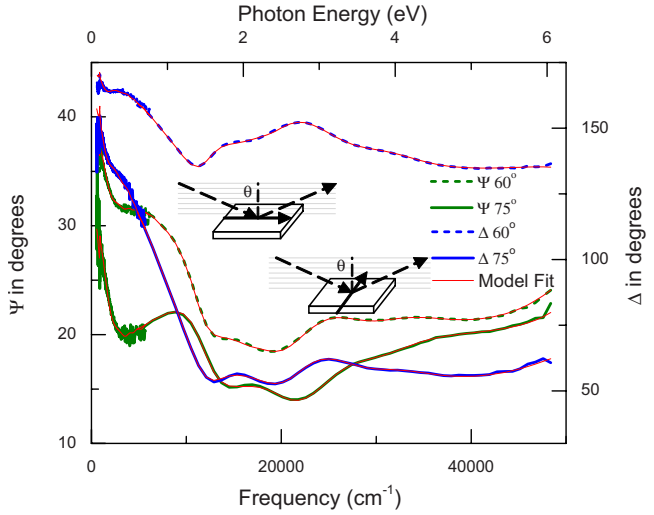

FIG. 1. (Color online) Room-temperature ellipsometry data for (110) CrO_2 film with c axis in the plane of incidence. Ψ and Δ were measured at incidence angles of 60° and 75°. The thin line shows the fit from the constructed model. Inset: schematic of the experimental geometry with c axis in the plane of incidence (top) and c axis perpendicular to plane of incidence (bottom). The dashed arrows represent the incident and reflected beams, with angle of incidence θ. The solid arrow indicates the direction of the c axis.

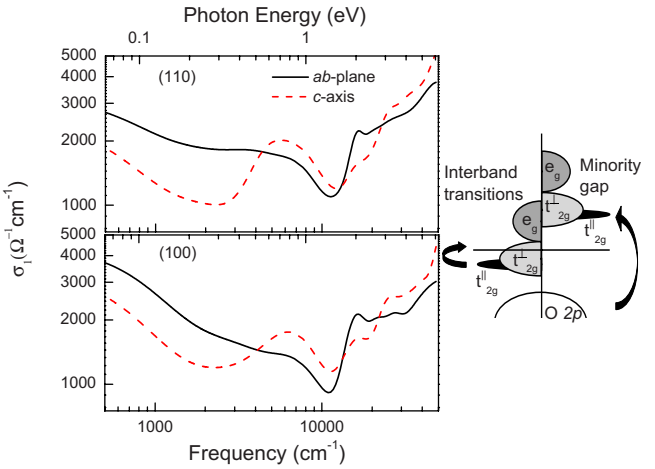

FIG. 2. (Color online) Real part of the optical conductivity of (110) CrO_2 (top panel) and (100) CrO_2 at room temperature in both ab plane and c axis directions. Right panel: sketch of the density of states of CrO_2 (Ref. 2).

anisotropy of this uniaxial crystal. The same model of the optical constants tensor has been employed to fit the four sets of experimental data for TiO_2 collected at 60° and 75° with the c axis both perpendicular and parallel to the plane of incidence. In this way we were able to obtain the conductivity for both the c axis and the ab plane of each of the two TiO_2 samples. Our data are in good agreement with those obtained in previous experiments.[21,22] To account for surface roughness in the substrate, we included in our model a top layer consisting of 50% void and 50% TiO_2 and described the response of such an effective layer with the Bruggeman effective-medium approximation.[23] The thickness of the layer was determined by the model fit to be 4 nm. Data for the CrO_2/TiO_2 films were modeled in a similar way. Specifically, we used the optical constants previously obtained for TiO_2 to characterize the substrate, so that the only fit parameters were the optical constants of CrO_2 in the c axis and ab plane directions. The CrO_2 layer of the model is composed of two separate sets of eight Kramers-Kronig consistent Gaussian oscillators[24] and a Drude function, amounting to 26 fit parameters. Two sets of oscillators are necessary because we want to describe the response along each of the two crystallographic directions. Figure 1 shows experimental data and the model fits for measurements of the (110) sample performed at room temperature with the c axis in the plane of incidence. It can be seen that our model provides good fits, within 5%, for the data at both angles throughout the entire experimental range.

III. RESULTS AND DISCUSSION

In order to analyze our results, it is useful to look at the real dissipative part of the optical conductivity, as it is related to the density of states. The complex optical conductivity can be obtained from the complex dielectric function using $\sigma(\omega)=\frac{i\omega[1-\epsilon(\omega)]}{4\pi}$. Figure 2 shows conductivity data for both CrO_2 samples at room temperature. The spectra show three main features: (i) a Drude contribution at low frequencies, (ii) a broad peak in the mid-IR region (0.2–1.5 eV), and (iii) a sharp onset of interband absorption at 1.5 eV indicative of a prominent band gap. Comparing our data with band-structure calculations[2,25] it is tempting to assign feature (iii) to transitions across the minority gap between the oxygen $2p$ and the chromium $3d$ bands, estimated by local spin-density approximation (LSDA) calculations to be 1.3 eV. Furthermore, transitions between the $t_{2g}^{\parallel}$ and the e_g levels (see right panel in Fig. 2) may contribute to absorption above 1.5 eV. Feature (ii) would correspond to interband transitions between the split t_{2g} levels. Based on this analysis, one might conclude that our data support the LSDA calculations more so than LSDA+U calculations. The latter include a Hubbard U term to account for intra-atomic Coulomb repulsion and predict a larger spin-minority gap of 2.1 eV, which is inconsistent with our results. While existing band-structure calculations are valid at very low temperatures, dramatic changes in the band structure are not expected at higher temperatures below T_C.

Data in Figs. 2–4 reveal significant anisotropy in the CrO_2 films throughout the entire frequency range of our measurements. Figure 3 shows dc conductivity, scattering rate $(1/\tau)$, and Drude plasma frequency (ω_p) data obtained from the Drude functions in our models. These spectral features are related to the Drude contribution of the optical conductivity by $\sigma_{\mathrm{Drude}}(\omega)=\frac{\omega_p^2}{4\pi(1/\tau-i\omega)}$. The plasma frequency we have obtained experimentally is somewhat lower than the LSDA prediction of ~2 eV.[26] At room temperature, the dc conductivity and the Drude plasma frequency in the ab plane are about 30% higher than in the direction of the c axis. Going back to Fig. 2 we note that this trend continues until about 0.5 eV. This is consistent with the knowledge that one of the $t_{2g}^{\perp}$ levels at the Fermi energy is hybridized with the oxygen $2p_y$

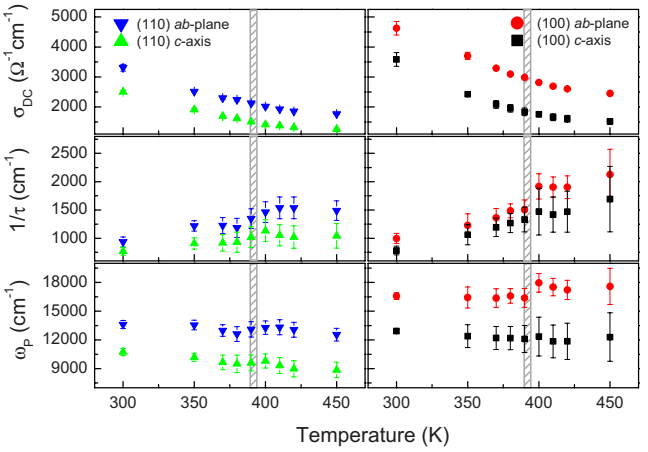

FIG. 3. (Color online) Dc conductivity (top), scattering rate, and Drude plasma frequency (bottom) as functions of temperature obtained from the Drude function in our model. The vertical bars indicate the Curie temperature. The left column shows data for CrO_2 on (110) TiO_2 and the right column is for CrO_2 on (100) TiO_2.

state forming a Π-type bond normal to the *c* axis.[14] In this way, some of the electrons at the Fermi energy can contribute to conductivity in the *ab* plane only. In the mid-IR region, the *c* axis conductivity shows a well-defined peak while in the *ab* plane conductivity we see a broad shoulder. At higher frequencies the anisotropy becomes smaller with the conductivity along both directions showing a rapid increase above 1.5 eV. In the *ab* plane response we see a more pronounced peak at 2 eV followed by a slower increase in conductivity at even higher energies. The response probed along the *c* axis direction reveals a more uniform increase in the conductivity, although peaks at 2 and 3 eV are still noticeable.

To further understand the band structure of CrO_2 it is crucial to study the temperature dependence of the conductivity, especially near T_C and across the ferromagnetic transition. Figure 4 shows temperature dependence of the optical conductivity for both films. It is important to note that the absorption region (iii) with onset at 1.5 eV exhibits virtually no temperature dependence, prevailing well above T_C. Noticeable temperature dependence is observed in the midinfrared region. In the case of the (110) film, the amplitude of this peak increases and its center becomes redshifted as temperature increases. In the (100) film we observe that, in the *c* axis direction, this peak broadens but its amplitude does not increase, while in the *ab* plane we see no clear peak in this region. The Drude free-carrier absorption at the lowest energies is modified as well. As shown in Fig. 3, the dc conductivity decreases and the scattering rate increases with increasing temperature. Above T_C, hints of saturation in the scattering rate are apparent, presumably due to the small electron mean-free path expected in the paramagnetic state.[26] The Drude plasma frequency remains approximately constant at all temperatures. This finding is in conflict with the double-exchange scenario of ferromagnetism in CrO_2 predicting a noticeable spectral weight transfer from high to low energy as temperature is reduced below T_C.[27] This expectation is substantiated by IR data for manganites, where the effective number of carriers decreases continuously with increased temperature, finally vanishing at T_C.[12] This result is also inconsistent with LSDA calculations predicting higher Drude plasma frequency in the paramagnetic state.[26] Similar behavior of the Drude plasma frequency across T_C is also found in ferromagnetic III-V semiconductors.[28,29] Dc conductivity in the *ab* plane remains higher than that in the *c* axis direction throughout our entire temperature range, with no discontinuous changes at T_C. These data are in good agreement with resistivity measurements performed on similar (100) CrO_2 samples.[15] We observe a higher scattering rate in the *ab* plane than in the *c* axis direction. From Fig. 3 we note that the dc conductivity of the (100) film is 30–35 % higher than that of the (110) film.

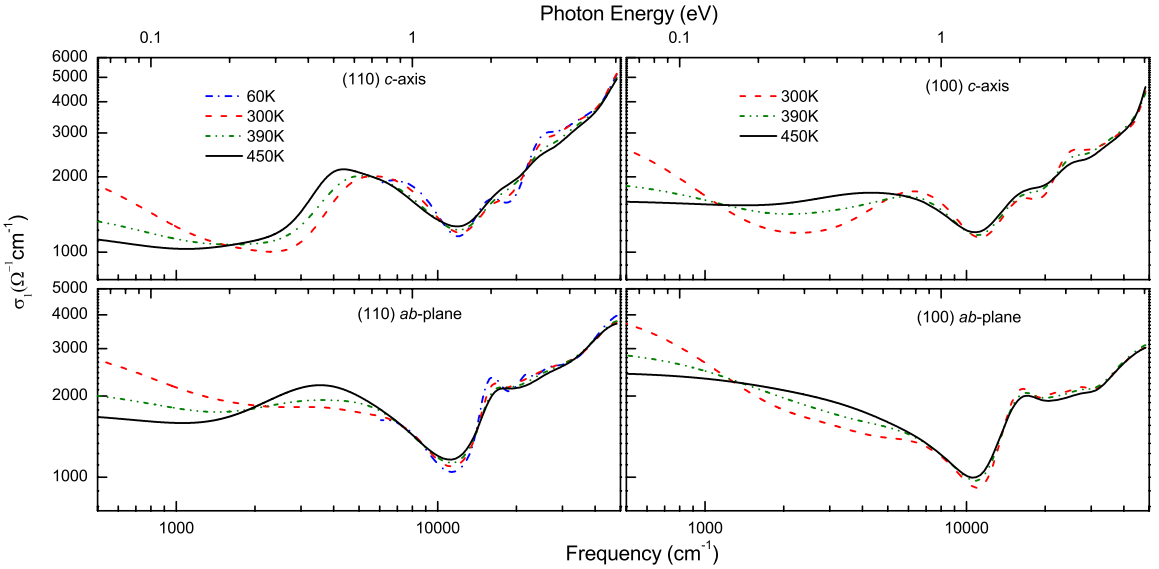

FIG. 4. (Color online) Optical conductivity in *ab* plane and *c* axis directions of each film at temperatures between 300 and 450 K for the (100) sample and between 60 and 450 K for the (110) sample.

An unanticipated result of our work is that we observe no significant changes either in the Drude absorption or in the interband resonance throughout the broad temperature range covering both the ferromagnetic and paramagnetic states. It is known that strain and strain-induced defects can affect the electronic and magnetic properties of thin films. This is a possibility in the (100) film, but not in the (110) film which has been shown to be strain-free.[16] Therefore, we expect to see a dramatic difference between the spectra at the low and high ends of our temperature range, the former corresponding to a fully spin-polarized ferromagnetic state well below T_C and the latter to a paramagnetic regime well above T_C. However, while the small peaks present at lower temperatures near 2 and 3 eV disappear quickly with increased temperature, the general trend of a sharp absorption starting at 1.5 eV remains unchanged. Therefore, assignment of the high-energy absorption to transitions across the minority gap of a half-metallic ferromagnet becomes problematic and is in disagreement with our results. The more noticeable temperature dependence in the mid-IR region might be explained by recalling that this peak could correspond to interband transitions between the split t_{2g} levels. As the temperature is increased and the sample enters the paramagnetic state, the minority-spin levels would presumably go down to the Fermi energy. This would allow excitations of minority spins into the conduction band with less energy, which could contribute to the broadening and increase in magnitude of this peak. In the case of the (100) film we expect the strain along the *b* axis to be greater than that along the *c* axis due to larger lattice mismatch in the direction of the *b* axis. Since the splitting of the t_{2g} levels is due to the elongation of the oxygen octahedra along the *c* axis,[3] one might expect that the way in which the t_{2g} levels split will be affected by this strain along the *b* axis, causing a difference in the conductivities of the two films in the mid-IR region. The lack of temperature dependence in the plasma frequency as well as in the sharp absorption region above 1.5 eV is in disagreement with the dramatic changes expected in the double-exchange scenario and in the current picture of the band structure of this material.

IV. CONCLUSION

We have obtained optical conductivity data for CrO_2 across the ferromagnetic transition at 390 K. The main features observed in our room-temperature data appear to be in good agreement with band-structure calculations for the fully spin-polarized ferromagnetic state. A study of the temperature dependence of the conductivity, however, poses new questions about the electronic band structure of this material. We see that the peak which, according to calculations, would correspond to transitions across the minority gap remains quite prominent at temperatures well above T_C. Furthermore, the Drude plasma frequency we obtained is temperature independent, which is inconsistent with the double-exchange scenario. We also observe an important anisotropy in the optical conductivity of CrO_2 and a difference in the conductivities of the two films. These observations are consistent with what is known about the crystal structure of this half-metal and about the strain in the films.

ACKNOWLEDGMENT

Work at UCSD was supported by ONR Contract No. N00014-08-1-0746.

*mstewart@physics.ucsd.edu

[1] K. Schwarz, J. Phys. F: Met. Phys. **16**, L211 (1986).
[2] A. Toropova, G. Kotliar, S. Y. Savrasov, and V. S. Oudovenko, Phys. Rev. B **71**, 172403 (2005).
[3] M. A. Korotin, V. I. Anisimov, D. I. Khomskii, and G. A. Sawatzky, Phys. Rev. Lett. **80**, 4305 (1998).
[4] Y. Ji, G. J. Strijkers, F. Y. Yang, C. L. Chien, J. M. Byers, A. Anguelouch, G. Xiao, and A. Gupta, Phys. Rev. Lett. **86**, 5585 (2001).
[5] A. Anguelouch, A. Gupta, G. Xiao, D. W. Abraham, Y. Ji, S. Ingvarsson, and C. L. Chien, Phys. Rev. B **64**, 180408(R) (2001).
[6] E. Z. Kurmaev, A. Moewes, S. M. Butorin, M. I. Katsnelson, L. D. Finkelstein, J. Nordgren, and P. M. Tedrow, Phys. Rev. B **67**, 155105 (2003).
[7] T. Tsujioka, T. Mizokawa, J. Okamoto, A. Fujimori, M. Nohara, H. Takagi, K. Yamaura, and M. Takano, Phys. Rev. B **56**, R15509 (1997).
[8] E. J. Singley, C. P. Weber, D. N. Basov, A. Barry, and J. M. D. Coey, Phys. Rev. B **60**, 4126 (1999).
[9] R. Yamamoto, Y. Moritomo, and A. Nakamura, Phys. Rev. B **61**, R5062 (2000).
[10] T. Yoshii, Y. Hamanaka, Y. Moritomo, and A. Nakamura, J. Lumin. **108**, 225 (2004).
[11] H. Huang, K. Seu, A. Reilly, Y. Kadmon, and W. F. Egelhoff, J. Appl. Phys. **97**, 10C309 (2005).
[12] Y. Okimoto, T. Katsufuji, T. Ishikawa, A. Urushibara, T. Arima, and Y. Tokura, Phys. Rev. Lett. **75**, 109 (1995).
[13] B. J. Thamer, R. M. Douglass, and E. Staritzky, J. Am. Chem. Soc. **79**, 547 (1957).
[14] C. B. Stagarescu, X. Su, D. E. Eastman, K. N. Altmann, F. J. Himpsel, and A. Gupta, Phys. Rev. B **61**, R9233 (2000).
[15] A. Gupta, X. W. Li, and G. Xiao, J. Appl. Phys. **87**, 6073 (2000).
[16] K. B. Chetry, M. Pathak, P. LeClair, and A. Gupta, J. Appl. Phys. (to be published).
[17] G. Miao, G. Xiao, and A. Gupta, Phys. Rev. B **71**, 094418 (2005).
[18] P. A. Stampe, R. J. Kennedy, S. M. Watt, and S. von Molnar, J. Appl. Phys. **89**, 7696 (2001).
[19] K. S. Burch, J. Stephens, R. K. Kawakami, D. D. Awschalom, and D. N. Basov, Phys. Rev. B **70**, 205208 (2004).
[20] M. M. Qazilbash, A. A. Schafgans, K. S. Burch, S. J. Yun, B. G. Chae, B. J. Kim, H. T. Kim, and D. N. Basov, Phys. Rev. B **77**, 115121 (2008).
[21] G. E. Jellison, Jr., F. A. Modine, and L. A. Boatner, Opt. Lett. **22**, 1808 (1997).

[22] T. Tiwald and M. Schubert, Proc. SPIE **19**, 4103 (2000).
[23] J. G. E. Jellison, Jr., L. A. Boatner, D. H. Lowndes, R. A. McKee, and M. Godbole, Appl. Opt. **33**, 6053 (1994).
[24] D. De Sousa Meneses, M. Malki, and P. Echegut, J. Non-Cryst. Solids **352**, 769 (2006).
[25] I. I. Mazin, D. J. Singh, and C. Ambrosch-Draxl, Phys. Rev. B **59**, 411 (1999).
[26] S. P. Lewis, P. B. Allen, and T. Sasaki, Phys. Rev. B **55**, 10253 (1997).
[27] L. Craco, M. S. Laad, and E. Müller-Hartmann, Phys. Rev. Lett. **90**, 237203 (2003).
[28] E. J. Singley, R. Kawakami, D. D. Awschalom, and D. N. Basov, Phys. Rev. Lett. **89**, 097203 (2002).
[29] E. J. Singley, K. S. Burch, R. Kawakami, J. Stephens, D. D. Awschalom, and D. N. Basov, Phys. Rev. B **68**, 165204 (2003).